

Fuzzy Theory-Based Partial Discharge Technique for Operating State Diagnosis of High-Voltage Motor

Hong-Chan Chang¹ · Shang-Chih Lin¹ · Cheng-Chien Kuo¹ · Chun-Yu Lin¹

Received: 2 December 2015 / Revised: 16 March 2016 / Accepted: 1 June 2016 / Published online: 13 June 2016
© Taiwan Fuzzy Systems Association and Springer-Verlag Berlin Heidelberg 2016

Abstract This study developed an operating state diagnostic system based on partial discharge detection for analyzing faults in high-voltage motor stator windings. First, the partial discharge signal of the stator windings is measured with a high-frequency current sensor, and then phase-resolved partial discharge technology is used to convert it into three-dimensional graphics. A systematic analysis process involving the use of fractal theory architecture for fault extraction from the signal characteristics was designed for identifying faults and obtaining the fractal dimension and the lacunarity of the characteristic parameters. Similarity function defined extension theory was used for building a failure signature database for each fault. Finally, to design and build fuzzy membership function and inference systems for analyzing the operation status of the motor, the partial discharge energy value and fault type were used as indicators in fuzzy algorithms. The experimental results prove that the fuzzy diagnostic system proposed in this paper is combined with the important information of fault type and discharge quantity, where fault type is successfully recognized, and a more reliable high-voltage motor operating state monitoring technique is created. The findings are expected to monitor the operating state of high-voltage motor more effectively, thus, reducing additional maintenance costs resulted from heavy accidents.

Keywords Partial discharge · High-voltage motor · Fractal theory · Extension theory · Fuzzy theory · Pattern recognition

1 Introduction

Most electrical equipment consists of conductive and insulating materials, and the insulating materials are particularly vulnerable, because when the electric field intensity in electrical equipment exceeds the electric field breakdown strength of the insulating materials, the equipment displays the random discharge phenomenon, which is known as partial discharge (PD) [1]. Furthermore, PD generating positions in an equipment are related to the positions of insulation materials [2]. Monitoring PD can help its early detection, leading to an increase in the service life of electrical equipment and enabling the immediate shutdown of the equipment for maintenance/repair. Nowadays, different devices, such as high-frequency current transformers (HFCTs), ultraviolet cameras, and ultra-high-frequency, high-voltage coupling capacitors (HVCCs), are used for measuring PD. The current study used a high-sensitivity HFCT for experimental measurements. Apart from being small and easy to carry, it facilitated subsequent data analysis. The motor signal ($NQ\Phi$) can be used for obtaining the phase spectrum. From a 3D graph, the number of PD pulses (N), PD magnitude (Q), and phase angle (Φ) of the PD data can be extracted from a complex image pattern using fractal theory [2, 3]; furthermore, a few crucial features can also be identified. Additionally, extension theory can be used for obtaining the parameters [4]. The most probable fault type can be determined by calculating the correlation index and obtaining a quantitative description of any of the elements

✉ Hong-Chan Chang
hcchang@mail.ntust.edu.tw

¹ Department of Electrical Engineering, National Taiwan University of Science and Technology, 43, Sec. 4, Keelung Rd., Taipei 10607, Taiwan

belonging to the domains associated with positive, negative, or zero [5–7]. The resulting fault type can be classified into four types on the basis of its severity, according to IEC 60034-27 standard [8]. In addition, many studies used partial discharge technology to evaluate the motor stator coil winding insulation state [9, 10]. This paper comprehensively considers partial discharge quantity and severity of fault defect by adopting the aforesaid literatures, and builds a more effective and complete stator winding state monitoring method. A motor can be protected from fault-related damage during operation if the severity of the fault is promptly identified, and PD studies have developed in the past, a diagnostic method in which the state of discharge operation, amount of partial discharge, and fault type of a motor can be determined. This method is more robust when the motor severity can be clearly identified from the PD generated. Finally, a fuzzy logic inference system can be used to determine the severity of a motor index by providing the type and amount of discharge of a motor as the two inputs and setting the proportion of their risk degrees [11]. The objective of the current study is to develop a method for determining the severity of a motor fault type. The determination of the severity can help in controlling the motor insulation conditions and enable the power industry to prevent early mechanical failure of test equipment enhance the stability of mechanical operation.

2 Background of Partial Discharge Technology

2.1 Test Environment and PD Equipment

The fault model tests conducted in this study required high-voltage power transmission equipment and protection devices. The test chamber was installed in a high-voltage room. The partial discharge detection system block diagram is as shown in Fig. 1. PD detection method used required a high voltage between the stator winding and the ground.

2.2 Introduction of PD Defect Model

According to the IEC 60034-27 standard, PDs can be divided into three main categories: internal discharge, slot discharge, and end-winding discharge. The following points include a description of these categories.

- *Internal voids* Internal PDs are generated within air or gas-filled pockets embedded in the stator winding insulation. PD processes in internal voids in solid insulation depend on many factors such as the void size and shape, gas in the void, gas pressure, and void surface chemistry which are all the causes of internal

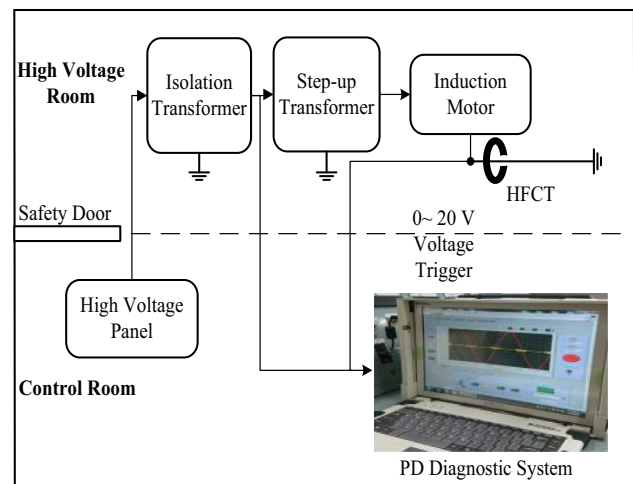


Fig. 1 Partial discharge detection system block diagram

cavity [12, 13]. The major cause of internal discharge in a normal environment is that it is difficult to avoid some hole gaps in the manufacturing process; however, these holes will not cause severe insulation aging, as it has low-level discharge quantity. The defect spectrum and discharge characteristic are as shown in Table 1.

- *End-winding discharge (Surface discharge)* Since surface discharges occur on the surface of the stator winding insulation, they are located in the end-winding section of a machine. Because the winding surface is usually corroded, semiconducting coating failure causes destruction of insulation. When the motor is running, it is impossible to avoid the dust and conducting particles in the air damaging the stator insulation, thus, the PD phenomenon is a normal condition. The defect spectrum and discharge characteristics are as shown in Table 1.
- *Slot discharge* Typically, these discharges appear only during machine operation and can corrode the semiconductive coating on stator bars, causing slot PDs and eventually phase-to-ground or phase-to-phase failure. Slot PD activity occurs when the electrical contact between the semiconductive coating of bars (or coils) and the magnetic core is poor. When a slot discharge occurs, meaning the stator end insulation has been severely degraded, the motor is significantly influenced, and the machine must be immediately shut down for repair and maintenance. The defect spectrum and discharge characteristics are as shown in Table 1 [14, 15].

2.3 Procedure of PD Test

In the high-voltage tests for PD measurements, the voltage step-up procedure conformed to IEC 60270. The PD signal

Table 1 Risk associated with the main PD sources in rotating machines [2, 8]

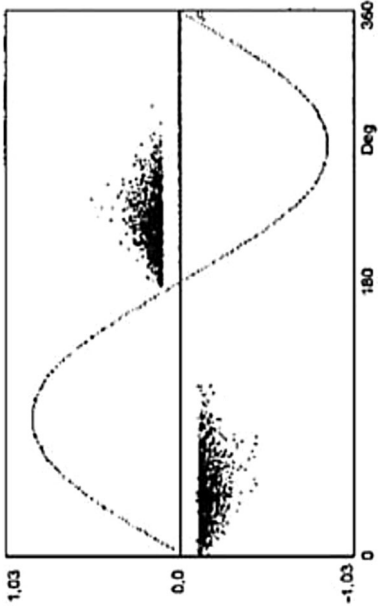
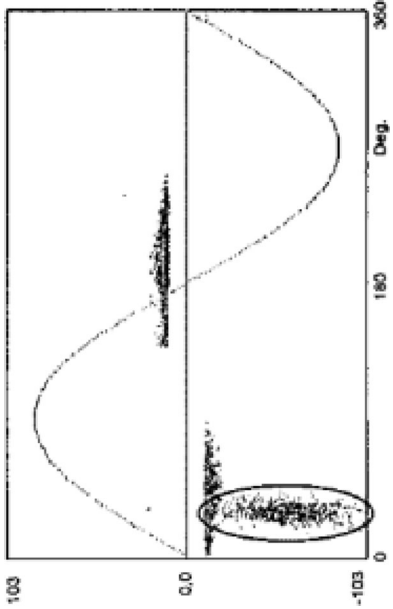
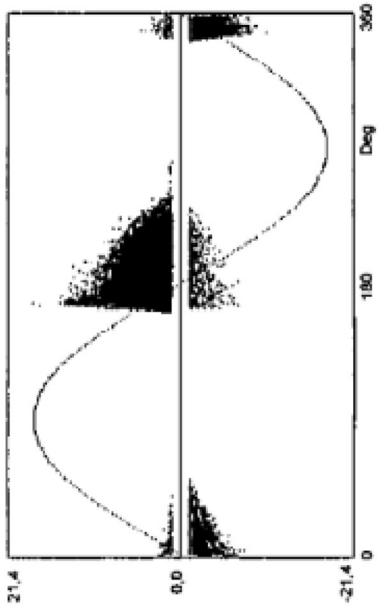
Partial discharge source	Risk	Pattern	Defect characteristics
Internal voids	Low		The first and third quadrants with a little amount of discharge The amount of discharge characteristics of the first and third quadrants of similar distribution
End-winding discharge (surface discharge)	Normal		The first quadrant discharge amount characteristics very similar to a tree The third quadrant with a little amount of discharge

Table 1 continued

Partial discharge source	Risk	Pattern	Defect characteristics
Slot discharge	High		<p>The discharge capacity in the third quadrant of the first quadrant is 1.5–2 times</p> <p>The discharge capacity of the third quadrant presented triangle</p>

is detected by a current transformer connected between the ground and the low-voltage electrode of the test object. Raw PD data were stored in a computer hard disk for the analysis with bespoke software.

3 Operating State Diagnosis System

Figures 2 and 3 show a block diagram of the setup used for PD detection and a flowchart of the process. PD fault characteristics were determined. The input signal acquisition steps should be well understood for accurately identifying the motor severity. The technical processes used in this study are as follows:

3.1 Signal Processing

In this experimental process, the sampling rate of the electrical signals for one power cycle (60 Hz) was set at 20 MS/s, and the power cycle time was 0.0166 s. For the partial discharge signal analysis, capturing three power cycle signals within 0.05 seconds through HFCT, and each signal cycle includes one million data. This study uses PRPD analytics [16] to observe the signal feature of partial discharge. First, the original signal of partial discharge is measured as shown in Fig. 4a. The signal is converted by MATLAB software into the 3D ($N-Q-\Phi$) phase pattern, and the numbers of discharge (N), discharge quantity (Q), and discharge phase (Φ) features of partial discharge are reviewed, as shown in Fig. 4b. Finally, the received data for subsequent analysis were based on the type of fault membership of the pattern correlation.

3.2 Feature Extraction Using Fractal Theory

This study uses the 3D probabilistic method to estimate the pattern of a partial discharge signal 3D spectrum random fractal surface, and creates the related functions and fractal dimensions of surface statistics. The partial discharge of the signal 3D spectrum is analyzed based on fractal theory, the corresponding x and y axes are the discharge phase angle and discharge quantity, and the corresponding z -axis is the numbers of discharge, in order to build the fractal surface. The random fractal surface of the partial discharge signal has the self-similarity and fractal characteristics of the fractal dimension, where the lacunarity index reflects the dissimilarity of denseness for recognition. Therefore, two feature parameters, fractal dimension and lacunarity, are analyzed, as shown in Fig. 5. The detailed procedure is as shown in Tables 1 and 2.

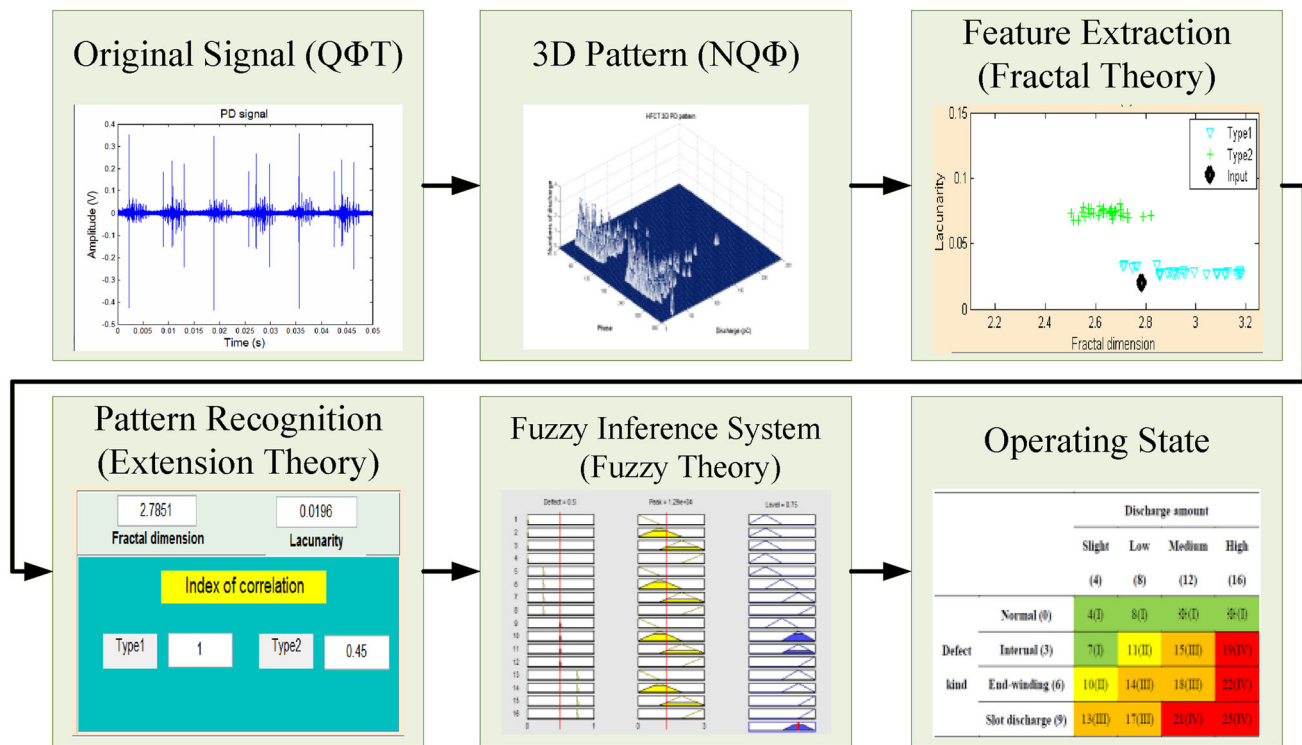


Fig. 2 Stator winding insulation condition diagnosis flowchart

$$n_s(i, j) = l - k + 1, \tag{1}$$

where l means the maximum numbers of discharge falls into No. l box, k means the minimum numbers of discharge falls into No. k box, and i, j are arbitrary numbers.

$$N_s = \sum_{i,j} n_s(i, j) \tag{2}$$

$$D = \frac{\log(N_s)}{\log(\frac{1}{s})}, \tag{3}$$

where $s = L/M$ is a scaling ratio.

$$p(m, L) = \frac{Q(m, L)}{N(L)}, \tag{4}$$

where $p(m, L)$ means there are m points in the box sized L , $Q(m, L)$ represents how many times the box moved each time and contains m points, N is the total occurrence number of point m in all moved boxes.

$$\sum_{m=1}^N p(m, L) = 1 \tag{5}$$

$$M(L) = \sum_{m=1}^N mp(m, L) \tag{6}$$

$$M^2(L) = \sum_{m=1}^N m^3 p(m, L) \tag{7}$$

$$A(L) = \frac{M^2(L) - [M(L)]^2}{[M(L)]^2} \tag{8}$$

3.3 Pattern Recognition Using Extension Theory

This technique is based on extension theory [5] and is used for fault pattern recognition in high-voltage motor stator winding insulation. First, a matter-element model is constructed for determining the fault type in high-voltage motor stator winding insulation. The fault type is then judged on the basis of the correlation membership from the correlation function characteristic values calculated for faults. The steps are presented in Table 3.

$$R_i = (N_i, C_j, V_{ij}) = \begin{bmatrix} N_i & c_1 & v_{i1} \\ & c_2 & v_{i2} \end{bmatrix}, \tag{9}$$

where $N_i = \{N_1, N_2, N_3, \dots, N_N\}$ is the i th defect type of the PD pattern. The classical domain $V_{ij} = \langle a_{ij}, b_{ij} \rangle$ of each value falls between the lower and upper bounds of the PD records, where a_{ij} represents the lower bound of the classic domains related to the j th input feature of the i th defect

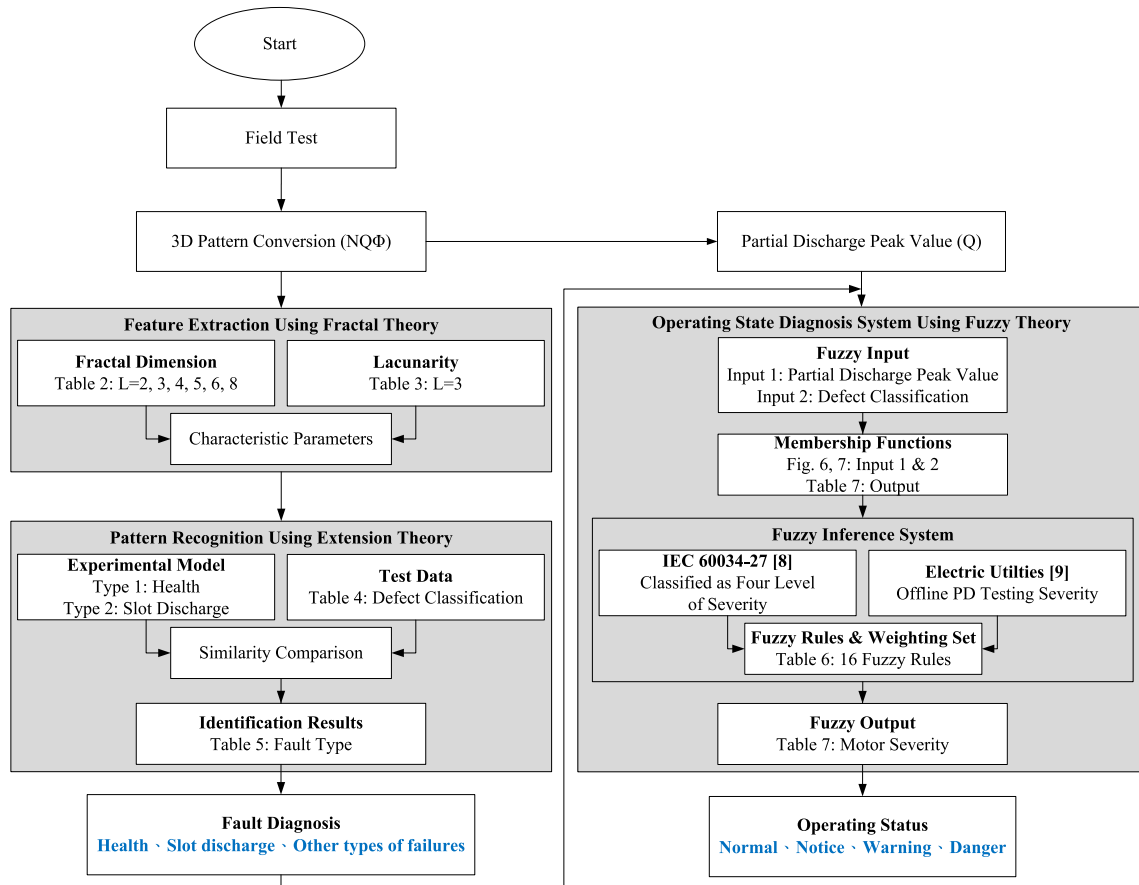


Fig. 3 The flowchart of fault diagnosis

type. In addition, b_{ij} of the upper bound of the classic domain is related to the j th input feature of i th defect type,

$$R_p = (N_p, C_j, V_{pj}) = \begin{bmatrix} N_p & c_1 & v_{p1} \\ & c_2 & v_{p2} \end{bmatrix} \quad (10)$$

$$K_i(x_j) = \begin{cases} \frac{-2\rho(x_j, X_{ij})}{|X_{ij}|}, & x_j \in X_{ij} \\ \frac{\rho(x, X_0)}{\rho(x_j, X_{pj}) - \rho(x_j, X_{pj})}, & x_j \notin X_{ij} \end{cases} \quad (11)$$

which relates the j th feature of the tested PD pattern to the j th input feature of the i th defect, as shown in step 1,

$$\sum_{j=1}^2 W_j = 1 \quad (12)$$

$$\zeta_i = \sum_{j=1}^2 W_j K_{ij}, \quad i = 1, 2, \dots, m \quad (13)$$

$$\lambda_i = \frac{2\zeta_i - \zeta_{\min} - \zeta_{\max}}{\zeta_{\max} - \zeta_{\min}}, \quad i = 1, 2, \dots, m, \quad (14)$$

where

$$\begin{cases} \zeta_{\max} = \max_{1 \leq i \leq 4} \{\zeta_i\} \\ \zeta_{\min} = \min_{1 \leq i \leq 4} \{\zeta_i\} \end{cases} \quad (15)$$

which falls between $[-1, 1]$ and is seen as a significant quantity for pattern recognition.

3.4 Operating State Diagnosis System Using Fuzzy Theory

This PD identification methods have been presented in previous papers [8–10], and its use in high-voltage motors is limited to determining the degree of risk from a single discharge amount or the extent of destruction from the type of motor failure defect on the basis of motor diagnostic system monitoring. Differing from the other diagnostic methods for partial discharge, this paper uses fuzzy calculation to make the rule base of a high-voltage motor, in order that the motor operating state can be judged more accurately. The detailed fuzzy algorithm is described in the next section.

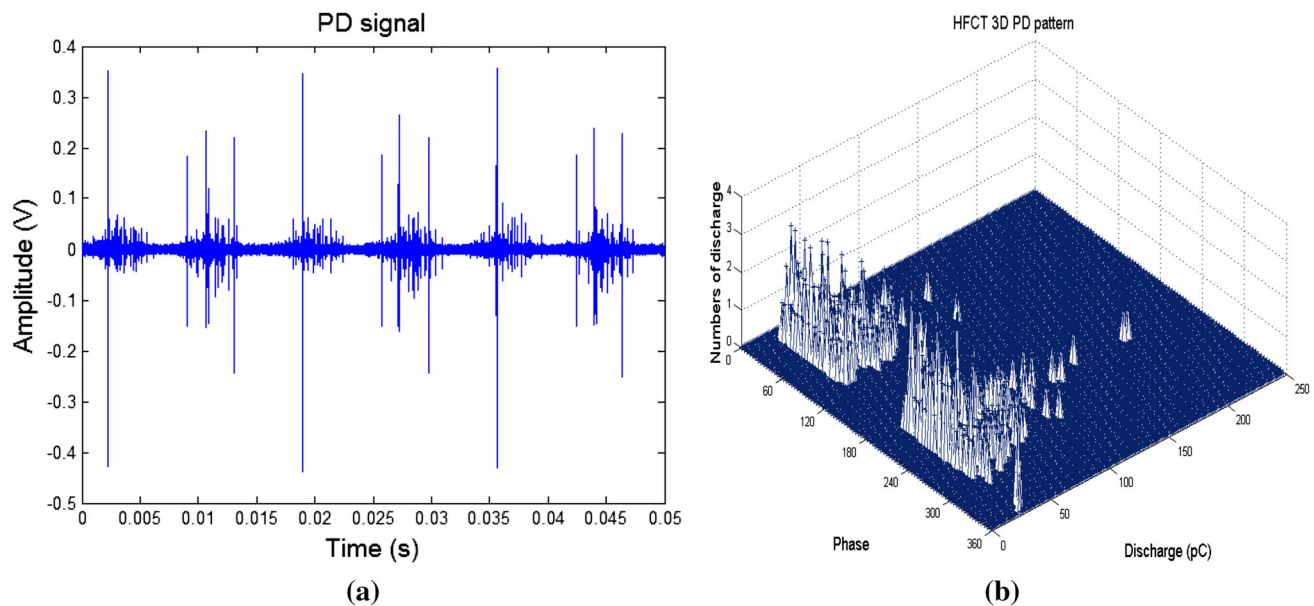


Fig. 4 **a** The original discharge pulse signal, **b** PD 3D ($N-Q-\Phi$) pattern

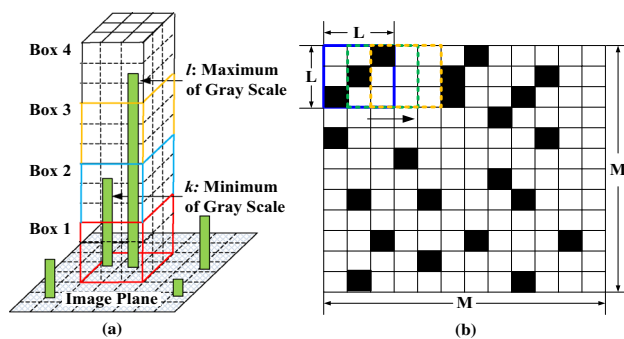


Fig. 5 Fractal theory: **a** The fractal dimension of the structure, **b** The lacunarity of the structure

According to the current offline discharge standard of an electric utility in Taiwan [9], there are four levels, as shown in Table 5. Using the categories, we developed a motor diagnostic system to judge the severity of faults.

Since the number of discharges and types of fault are major characteristics of PDs, these two indices were provided as the two inputs to a fuzzy inference system (FIS) [17]. First, the discharge amount was set as the first input. The standard range of regulation values of an electric utility was used to construct a working fuzzy membership function, as shown in Fig. 6. The design of membership function is divided into four conditions according to the intensity discharge amount (Table 5). The severity of slight discharge is 0–0.33, and the weight decreases as the severity increases; the low and medium membership functions are designed as a triangle, and the severity range is 0–0.66 and 0.33–1, respectively. When the value is 0.33

and 0.66, the low and medium discharge quantities have the maximum weight, respectively. When the discharge quantity is high and the severity is 0.66, the weight is maximized linearly. PD faults were used as the second input, and the types of diagnostic system settings were used to construct a fuzzy membership function, as shown in Fig. 6.

The identification of a PD pattern can indicate the type of fault. In the current study, a motor was monitored online for three main types of discharges (slot discharge, end-winding discharge, and internal voids). The membership function of defect type is determined by referring to IEC 60034-27 [8], and the severity of different defects can be known. One single fault type is used for diagnostic analysis in this paper, thus, it is not a composite defect model. Therefore, in the determination of membership function, the location of each defect is defined according to the severity of the defect type. Where severity includes health, internal voids, and end-winding discharge to the most severe slot discharge. The membership functions are a straight line, and the corresponding locations are 0, 0.25, 0.5, and 0.75, respectively, as shown in Fig. 7.

The weights of two input ends are set, the discharge quantity is classified into the following four levels, and the weights corresponding to the discharge quantities in ascending order are 4, 8, 12, 16. The weight of the other input end is distributed by referring to the fault severity established in [8], in order to discuss the effect of health, internal voids, end-winding discharge, and slot discharge in different positions on the state of insulation. The weight is set as 0 for insulated winding in the healthy condition,

Table 2 Detailed flow of fractal dimension

Step	Explanation
1	Assuming the image plane to be a $M \times M$ gray-level matrix, divide the 3D space into $L \times L \times L'$ boxes
2	Select size L of different boxes, this study selects $L = 2,3,4,5,6,8$
3	Calculate the number of boxes for different box sizes, expressed as (1)
4	Calculate the number of boxes for the overall image intensity surface, expressed as (2)
5	Use linear least squares fit, $\{[\log(\frac{1}{s}), \log(N_s)]\}$, to calculate fractal dimension D , expressed as (3)

Table 3 Detailed flow of lacunarity

Step	Explanation
1	Assuming the spectrum to be $M \times M$ binary image, and covered with box in edge length of $L \times L$
2	Move the box to the binary image for sampling, calculate the frequency distribution, represented by probability as (4), as shown in Fig. 7b
3	Normalize $p(m, L)$, make the total probability of frequency distribution 1, and (5) is obtained
4	Calculate first-order momentum $M(L)$ and second-order momentum $M^2(L)$ according to statistical moments, expressed as (6) and (7)
5	Work out lacunarity Δ from the first-order and second-order momentums, calculated by (6) and (7), expressed as (8)

while the weights of other types are defined as 3, 6, and 9 according to the severity. Therefore, the row–column weight ratio is 4:3. The weight settings are as shown in Table 6, and there are 16 states, where the numbers corresponding to row and column are added up. Each cell obtains the result of the operating state according to the corresponding color in the cell. When the stator winding is “Health”, whatever the discharge quantity is, it is a healthy state. When the stator winding has an internal void defect, which is difficult to be avoided in the process, the motor operating state varies with the discharge quantity. When the stator winding has an end-winding defect, it means this motor has been considerably damaged. When the discharge quantity is “Low”, the operating state has reached the “Warning” level. When the stator winding has a slot discharge defect, the motor stator insulation has been severely damaged. Even if the discharge quantity is “Slight”, the operating state has reached the “Warning” level. In terms of output, the weights in Table 6 are defuzzified and normalized to obtain the output range, as shown in Table 7. An output of <0.32 is “Normal”; 0.36–0.48 is “Notice”; 0.52–0.72 is “Warning”; 0.76–1 is “Danger”. All probabilities are in this interval.

At present, the PD method is mostly used to identify the motor stator winding insulation state, and the discharge quantity is used as the main index to evaluate operating risk. While this action can easily monitor the state, it is unlikely to detect potential risks. For example, when a PD signal of an instantly high amplitude value is measured, it may be resulted from ambient noise or temperature anomaly, rather than insulation degradation. On the other hand, after long operation, the insulating property of the motor ages gradually due to external factors. The PD amount is relatively apparent at the initial stage of aging; however, at the late stage of aging, PD amount decreases gradually, and the operating state is likely to be misrecognized as a normal state. Based on this, this paper combines the fuzzy inference system with the intensity discharge amount and defect type of partial discharge in order to evaluate the high-voltage motor operating state. However, in current partial discharge technology, comprehensive diagnosis is seldom discussed. Therefore, this paper designs an insulating property assessment criterion suitable for the power company and IEC 60034-27 recommended fuzzy system, in order to build a high-voltage motor operating state monitoring system.

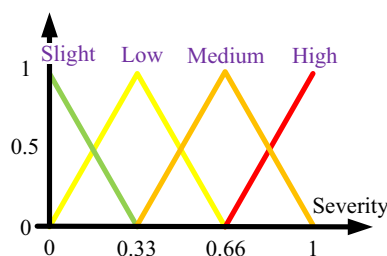


Fig. 6 Membership function of discharge amount

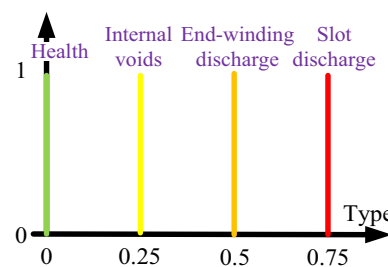


Fig. 7 Membership function of PD defect type

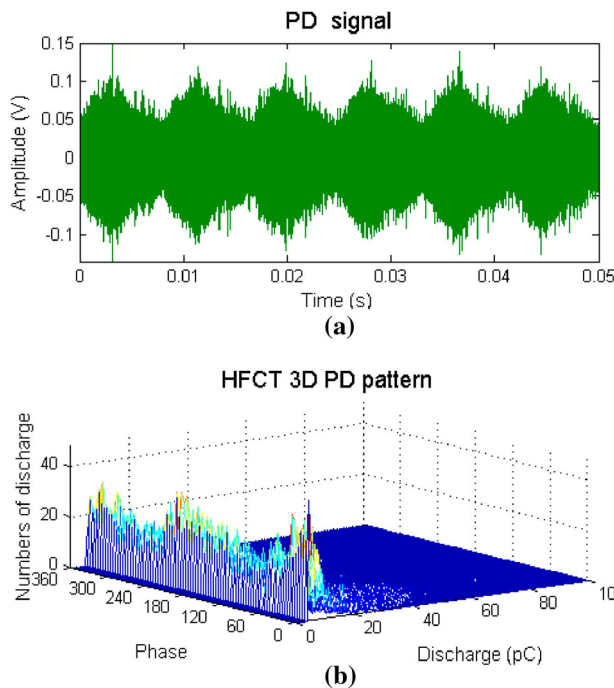


Fig. 8 **a** The actual healthy motor measuring signal, **b** PD 3D pattern

After constructing the fuzzy membership function, we constructed a complete set of fuzzy rules. On the basis of the severity of motor faults in Table 6, 16 multi-input processing rules were framed for each input feature, and they were changed several times through trial and error. The results of the FIS are presented by the next section.

4 Illustrative Examples

A discussion of experimental results for a healthy stator coil and slot discharge faults is presented in this section. In each case, the original pulse signal diagram is obtained and compared with the $NQ\Phi$ pattern of the IEC standard. The severity of the motor fault is judged from the fault type and discharge amount, which are regarded as fuzzy inputs. This paper designs two cases for discussion, the risk level is evaluated for the operating state, the operating state of a

high-voltage motor can be monitored more accurately, and system reliability is effectively enhanced.

4.1 Example 1_Healthy Type

Figure 8a shows the original pulse signal of partial discharge, as obtained by measuring a healthy motor. The motor is provided by a power company, and the $NQ\Phi$ pattern, as derived from the observed pattern discharge characteristics, as shown in Fig. 8b. The red and yellow colors imply a larger number of discharges.

Figure 9 shows the fault type obtained at the GUI interface using fractal and extension theories. The fractal dimension (X -axis) and lacunarity (Y -axis) feature values are obtained from the test data by the fractal method, and the two defect types can be apparently distinguished. Fractal function blocks can be seen at the input point (represented as “◆”) located in the type 1 range (represented as “▽”). Then type 2 represented by “+” cluster above the type 1. Two kinds of defect types can easily identify in fractal block. Furthermore, the extension of correlation index shows the highest correlation for type 1 (index value of 1). Different from type 1 of index correlation get the -1 value. Through the extension theory correlation analysis to determine the type of motor is healthy. The analysis result is used as the input of the FIS for evaluating the operating state.

According to the high-voltage experimental measurement, the discharge quantity is 53.57 pC, and the discharge quantity severity corresponding to Table 5 is Slight. In order to judge the motor operating state more accurately, differing from aiming at the discharge quantity or defect type in the past, this paper uses fuzzy system calculus involving the fault type (Health: 0) and PD amount (Slight: 4), which shows that the motor belonged to the “Normal (4)” state in Tables 6 and 7. Table 7 shows the set of motor severity indices, and the condition of the motor and preset experiment results agree with each other. Therefore, the high-voltage motor is defectless. Motor monitoring continues to be sustainable, without requiring the motor inspection to be terminated.

Table 4 Detailed flow of extension theory

Step	Explanation
1	Formulate the matter element R_i , ($i = 1, 2, \dots, m$) for each defect type, expressed as (9)
2	Extract the PD features as fractal dimension and lacunarity. Each defects test model of feature magnitude can be expressed as (10)
3	Calculate the degree of correlation $Ki(x_j)$ through (11) for each test model
4	Set the weights of PD features W_1 and W_2 in the process. In this work, as show in (12), both weights are equal to 0.5
5	Calculate the indices of correlation for each defect type, expressed as (13)
6	The indices of correlation normalized into an interval $[-1, 1]$ as (14). This process is seen as a significant quantity for pattern recognition
7	Find the maximum index of correlation of the following formula. In case ($\lambda_k = 1$), the tested model is determined as the k th defect type

Table 5 Partial discharge off-line test discharge severity index

Discharge amount (pC)	Condition
<10,000	Slight
10,000–20,000	Low
20,000–30,000	Medium
>30,000	High

Table 6 Evaluate the fuzzy inputs and the fuzzy rule base

		Discharge amount			
		Slight (4)	Low (8)	Medium (12)	High (16)
Defect type	Health (0)	4(I)	8(I)	*(I)	*(I)
	Internal voids (3)	7(I)	11(II)	15(III)	19(IV)
	End-winding discharge (6) (surface discharge)	10(II)	14(III)	18(III)	22(IV)
	Slot discharge (9)	13(III)	17(III)	21(IV)	25(IV)

© The “*” operating state in Table 6 represents the level of “Normal”. Theoretically, when the model recognition result is normal, such an abnormally high discharge quantity will not be measured; therefore, a sharp increase in discharge quantity may be resulted from ambient noise or external factors. As this discharge is not caused by stator insulation degradation, it is identified as a “Normal” type

4.2 Example 2_Slot Discharge Type

The fault data for a fault in a power plant in Taiwan was obtained; the power plant contained repaired 13.8 kV, 9.7 kVA generators. The actual situation is an exception occurring during motor operation, and during the maintenance of the stator winding slot region, a white powder was formed. Therefore, this experiment only implements single-phase boosting for the stator part to check whether the

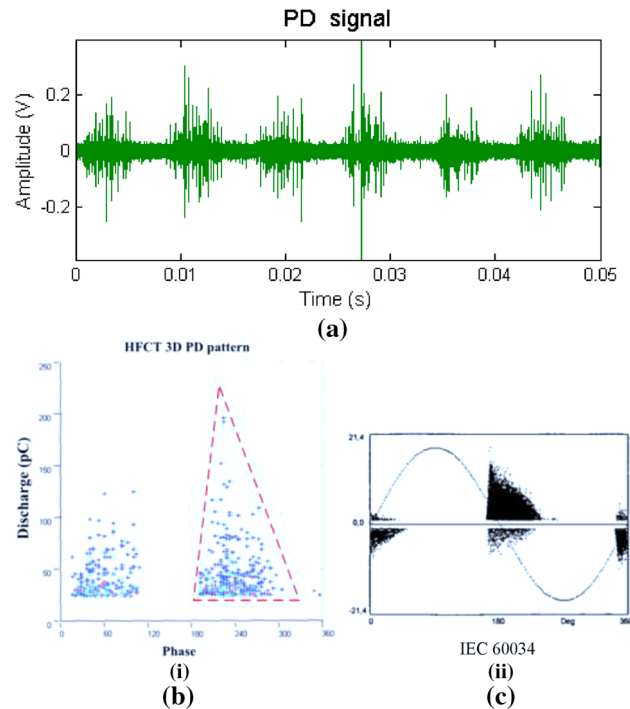


Fig. 10 a The actual motor original signal, b (i) The actual $NQ\Phi$ pattern (ii) International standard $NQ\Phi$ pattern

measurement signal has insulation deterioration in the stator slot (Fig. 10).

The original pulse signal is shown in Fig. 10a. All IEC 60034-27 standard patterns were compared with $NQ\Phi$ patterns, and the fault type was determined. Figure 10b(i) shows an IEC 60034-27 standard pattern, and a slot discharge fault pattern in Fig. 10b(ii) can be observed. The third quadrant discharge amount is 1.5–2 times the first quadrant discharge amount, and the initial discharge of the third quadrant shows a sharp rise. The two patterns are compared to determine whether their signal had PD characteristics and whether the discharge pattern was consistent with the slot discharge fault standard pattern.

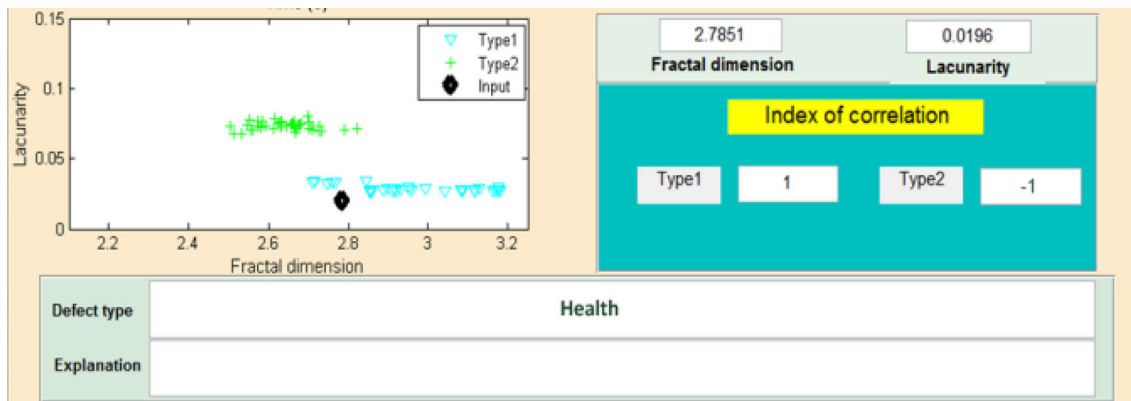


Fig. 9 Defect type diagnosis results—Health

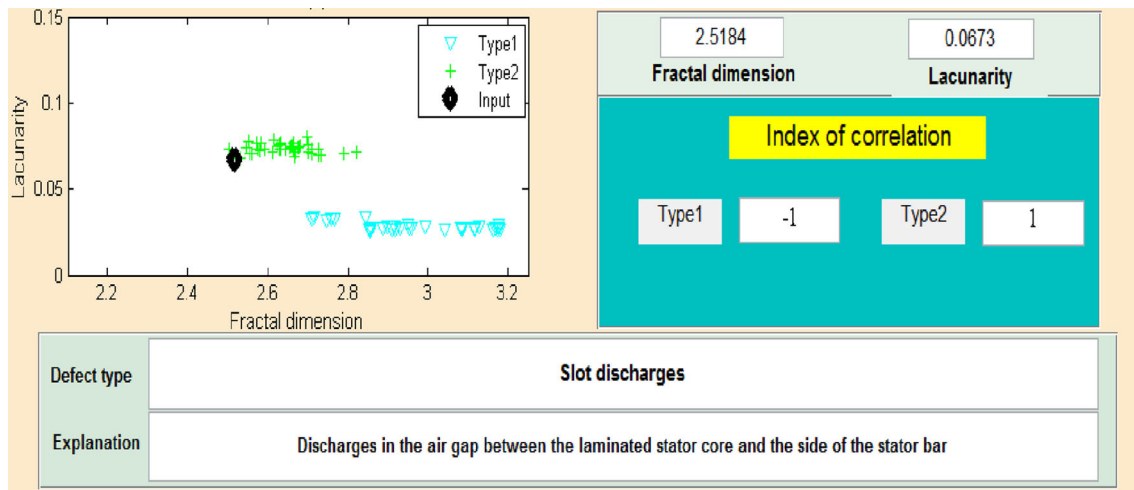


Fig. 11 Defect type diagnosis results—Slot discharge

Fractal function blocks have two types, One is healthy type (represented by “ ∇ ”), the other is slot discharge (represented by “+”). The data input (represented by “ \blacklozenge ”) is located in type 2 in Fig. 11. In extension function blocks, the correlation of the index values can be seen as the highest type 2 (index value of 1). According to the input, type 2 index values were located farther from type 1 group, and the index sequentially decreased (minimum value of -1), implying the slot discharge type of motor fault. However, the partial discharge quantity is 140 pC in the test, which is slight, and corresponds to Table 5 offline discharge degrees. The intensity discharge amount (Slight: 4) and fault type (Slot Discharge: 9) were obtained using a fuzzy system for internal operation. It can be ascertained whether the high-voltage motor has reached the fourth level corresponding to the level of “Danger (13)” shown in Tables 6 and 7. The experimental results confirmed that the type of slot discharges, if only the amount of partial discharge to predict the motor status will be mistaken for “Normal”. However, when the fuzzy system is used for analysis, it shows that the motor operating state has reached the “Warning” level. Therefore, it is proved that, the operating state evaluation method proposed in this paper can effectively detect motor error state, and suggests overhaul scheduling, in order to avoid more severe consequences (Table 7).

Table 7 Fuzzy output and risk level of operation states

Output level	Operation states
(I) <0.32	Normal
(II) $0.36\text{--}0.48$	Notice
(III) $0.52\text{--}0.72$	Warning
(IV) $0.76\text{--}1$	Danger

5 Conclusion

In this study, the PD of a high-voltage motor was measured, and a motor fault model based on the stator fault types was constructed using HFCT capture signals obtained during the application of a voltage. The fault type of the signal obtained from the pattern measurement results is discussed, and the analysis of the results showed that a PD fault database can be built. The system should be strengthened for motor stator insulation fault identification. In addition, this paper uses fuzzy theory to successfully build an expert system, which is combined with the current partial discharge quantity, strength specifications of electric utility, and fault type severity specifications of IEC 60034-27, thus, this operating state monitoring system has higher reference value. According to the illustrative examples, when the slot discharge phenomenon causes insulation aging, the discharge quantity is slight. Based on the analysis of this system, the operating state can be effectively pre-warned, in order to avoid more serious accidents, and heavy losses of lives and economy. In future research, the operating states of high-voltage motors will be evaluated by online monitoring techniques, in order to further validate the reliability of the state monitoring method proposed in this paper.

Acknowledgments The research was supported by the Ministry of Science and Technology of the Republic of China, under Grant No. MOST 103-2221-E-011-077-MY2.

References

1. IEC: High-voltage test techniques—partial discharge measurements. IEC 60270 (2001)

2. Hudon, C., Bélec, M.: Partial discharge signal interpretation for generator diagnostics. *IEEE Trans. Dielectr. Electr. Insul.* **12**(2), 297–319 (2005)
 3. Satish, L., Zaengl, W.S.: Can fractal features be used for recognizing 3-D partial discharge patterns? *IEEE Trans. Dielectr. Electr. Insul.* **2**(3), 352–359 (1995)
 4. Gu, F.C., Chang, H.C.: Gas-insulated switchgear PD signal analysis based on Hilbert-Huang transform with fractal parameters enhancement. *IEEE Trans. Dielectr. Electr. Insul.* **20**(4), 1049–1055 (2013)
 5. Cai, W.: The extension set and incompatibility problem. *J. Sci. Explor.* **1**(1), 81–93 (1983)
 6. Cavallini, A., Montanari, G.C., Puletti, F., Contin, A.: A new methodology for the identification of PD in electrical apparatus: properties and applications. *IEEE Trans. Dielectr. Electr. Insul.* **12**(2), 203–215 (2005)
 7. Chao, K.H., Chen, P.Y.: An intelligent fault diagnosis method base on extension theory for DC-AC converters. *Int. J. Fuzzy Syst.* **17**(1), 105–115 (2015)
 8. IEC: Off-line partial discharge measurements on the stator winding insulation of rotating electrical machines. IEC 60034-27 (2006)
 9. Zeng, B.Q.: Discussion on the issue using the generator coil of the PD source detection. *Taiwan Power Company Eng. J.* **2**, 27–40 (2010)
 10. Renforth, L.A., Hamer, P.S., Clark, D.: High-voltage rotating machines: a new technique for remote partial discharge monitoring of the stator insulation condition. *IEEE Ind. Appl.* **20**(6), 79–89 (2014)
 11. Chang, J.H., Lee, H.H.: A study on reliability based assessment algorithm for high voltage induction stator windings. In: *Proceedings of the IPMHVC Conference*, pp. 600–603 (2012)
 12. Ueta, G., Wada, J., Okabe, S., Miyashita, M., Nishida, C., Kamei, M.: Insulation characteristics of epoxy insulator with internal delamination-shaped micro-defects. *IEEE Trans. Dielectr. Electr. Insul.* **20**(5), 1851–1858 (2013)
 13. Ueta, G., Wada, J., Okabe, S., Miyashita, M., Nishida, C., Kamei, M.: Insulation characteristics of epoxy insulator with internal void-shaped micro-defects. *IEEE Trans. Dielectr. Electr. Insul.* **20**(2), 535–543 (2013)
 14. Liese, M., Brown, M.: Design-dependent slot discharge and vibration sparking on high voltage windings. *IEEE Trans. Dielectr. Electr. Insul.* **15**(4), 927–932 (2008)
 15. Song, J., Li, C., Lin, L., Lei, Z., Bi, X.Y.: Slot discharge pattern of 10 kV induction motor stator coils under condition of insulation degradation. *IEEE Trans. Dielectr. Electr. Insul.* **20**(6), 2091–2098 (2013)
 16. Strachan, S.M., Rudd, S., Judd, M.D.: Knowledge-based diagnosis of partial discharges in power transformers. *IEEE Trans. Dielectr. Electr. Insul.* **15**(1), 259–268 (2008)
 17. Sureshjani, S.A., Kayal, M.: A novel technique for online partial discharge pattern recognition in large electrical motors. In: *Proceedings of the ISIE Conference*, pp. 721–726 (2014)
- Hong-Chan Chang** (M'87) was born in Taipei, Taiwan on 5 March 1959. He received the B.S., M.S., and Ph.D. degrees, all in Electrical Engineering, from National Cheng Kung University in 1981, 1983, and 1987, respectively. In 1987 he joined the National Taiwan University of Science and Technology (NTUST), Taipei, Taiwan, as a faculty member. He is presently a Professor and formerly served as the vice president of NTUST. His major areas of research include pattern recognition, partial discharge, and application of artificial intelligence to power systems.
- Shang-Chih Lin** was born in Taichung, Taiwan on 9 May 1988. He is currently a Ph.D. candidate in the Department of Electrical Engineering of the National Taiwan University of Science and Technology (NTUST). He received the B.S. and M.S. degrees from the Nan Kai University of Technology (NKUT) in 2010, and 2012, respectively. His research interests include fault diagnosis, pattern recognition, optimization algorithms, and economic dispatch.
- Cheng-Chien Kuo** (M'01) was born in Yunlin, Taiwan on 9 August 1969. He received the B.S., M.S., and Ph.D. degrees all in Electrical Engineering, from the National Taiwan University of Science and Technology (NTUST) in 1991, 1993, and 1998, respectively. He has been with National Taiwan University of Science and Technology (NTUST) since 2015, where he is currently a Professor in the Department of Electrical Engineering. His research interests include microprocessor, energy management system, and optimization techniques, and partial discharge.
- Chun-Yu Lin** was born in Taipei, Taiwan on 25 Dec 1991. He is currently a master student in the Department of Electrical Engineering of the National Taiwan University of Science and Technology (NTUST). He received the B.S. degrees from National Yunlin University of Science and Technology in 2014. His research interests include fault diagnosis, pattern recognition, and fuzzy algorithm.